2013

Spectroscopic Study of Charge Transfer Induced Blue Shifting of Pyrimidine/Water Mixtures on Silver Substrate

Annie Katherine McClellan
University of Mississippi. Sally McDonnell Barksdale Honors College

Spectroscopic Study of Charge Transfer Induced Blue Shifting of Pyrimidine/Water Mixtures on Silver Substrate

By:
Annie Katherine McClellan

A thesis submitted to the faculty of The University of Mississippi in partial fulfillment of the requirements of the Sally McDonnell Barksdale Honors College.

Oxford
May 2013

Approved by

_____
Advisor: Professor Nathan Hammer

_____
Reader: Professor Gregory Tschumper

_____
Reader: Professor Susan Pedigo

ACKNOWLEDGEMENTS

Many people here at the University of Mississippi have supported me throughout the time I worked on the research presented in this manuscript. I would like to thank the professors of the Department of Chemistry and Biochemistry for supporting me throughout my undergraduate career and challenging me to become a better student and chemist. I would also like to thank the members of my research group, specifically Dr. Debra Jo Sage and Dr. Ashley Wright, for their support throughout this research endeavor. Lynn Joe, a fellow researcher and friend, deserves special thanks for aiding in the experimental procedures during this project as well as performing the Lorentzian fits. Lastly, I would like to thank my advisor, Dr. Nathan Hammer for allowing me to work in this research group over the past few years as well as preparing me for my future in the chemical sciences.

ABSTRACT
ANNIE KATHERINE MCCLELLAN: Spectroscopic Study of Charge Transfer Induced Blue Shifting of Pyrimidine/Water Mixtures on Silver Substrate
(Under the direction of Dr. Nathan Hammer)

Surface enhanced Raman spectroscopy (SERS) is a chemical method gaining much popularity in recent years. With the use of a roughened metal surface or metal nanoparticles, surface plasmon resonances enhance the electromagnetic field allowing for increased Raman signal. Pyrimidine, having two lone pairs of electrons, is capable of charge transfer interactions contributing to a SERS chemical enhancement factor as well. It has recently been reported that hydrogen bonding with water results in the blue-shifting of certain normal modes of pyrimidine. By comparing experimental polarized Raman spectra with the results of electronic structure calculations, the origin of this blue-shifting was found to center around charge transfer from pyrimidine to water in the bulk mixtures.

In this thesis, we show how weak, noncovalent interactions affect the SERS spectra of neat pyrimidine and pyrimidine solutions of both water and methanol using silver-island film substrates. We analyze the spectroscopic results by comparing both the Raman and SERS spectra of bulk pyrimidine and pyrimidine/solvent mixtures to theoretical predictions in order to deduce the mechanisms of the spectral shifts. SERS spectra of pyrimidine and pyrimidine solutions exhibit blue shifts in ν_1 and ν_{8b} and a red shift at ν_{8a} due to charge transfer and the chemical enhancement from the silver island films. Multiple components in ν_1's spectra correspond to free pyrimidine, and one or two interactions with nitrogen atoms. Comparison of the experimental spectra suggests that interactions between pyrimidine and silver dominate interactions between pyrimidine and the solvent molecules. The magnitude of the blue shifts suggests charge transfer on the order of 35 and 80 milli electrons for one or two interactions, respectively.

TABLE OF CONTENTS

Acknowledgments…… *iii*
Abstract…… *iv*
List of Figures and Tables…… *vii*

Chapter 1: Spectroscopic Methods……. 1

1.1 Spectroscopy Overview…….. 1

1.1.1 Electromagnetic Radiation…….. 1

1.1.2 Quantum Mechanics……..… 4

1.2 Vibrational Spectroscopy……... 5

1.3 Raman Spectroscopy……..… 7

1.4 Surface Enhanced Raman Spectroscopy……..… 11

Chapter 2: Pyrimidine……... 14

2.1 Biological Importance……..… 15

2.2 Previous Studies…… 17

2.2.1 Hydrogen Bonding Effects on Pyrimidine…… 18

2.2.2 Micro-Hydrated Pyrimidine Structures……..… 19

2.2.3 Normal Modes of Crystalline Pyrimidine.…… 19

2.2.4 Charge Transfer Mechanism of SERS……..… 20

Chapter 3: Vibrational Spectroscopy of Pyrimidine and Pyrimidine Mixtures to Analyze Charge Transfer Induced Shifts…..…… 23

3.1 Introduction……..… 23

3.2 Experimental Procedures…….. 25

3.3 Results and Discussion……. 26

3.3.1 Modes ν_{6a} and ν_{6b}……. 28

3.3.2 Modes ν_9, ν_{15}, and ν_3……,…… 29

3.3.3 Modes ν_1 and Fermi Resonance $\nu_{10b} + \nu_{16b}$……..……. 31

3.3.4 Modes ν_{8a} and ν_{8b}…….. 36

3.3.5 Comparison to Theory…….…. 38

3.4 Conclusions……..…...… 41

List of References……..……...…… 42

LIST OF FIGURES AND TABLES

Figure 1.1 Einstein coefficients for absorption and emission……..……. 2

Figure 1.2 Possible transitions caused by electromagnetic radiation…….… 6

Figure 1.3 Schematic of Rayleigh and Raman scattering…….. 9

Figure 2.1 The three diazines molecules……..… 14

Figure 2.2 Natural occurring pyrimidine derivates prevalent in biological systems..... 16

Table 2.1 Normal modes of pyrimidine and pyrimidine/water mixture…….. 18

Table 2.2 Normal modes of liquid and crystalline pyrimidine…… 20

Table 2.3 Vibrational frequencies of pyrimidine and pyrimidine solution……..... 21

Table 3.1 Raman and SERS normal modes of pyrimidine and pyrimidine mixtures….. 27

Table 3.2 Shifts from pure pyrimidine Raman modes…….……..… 27

Figure 3.1 ν_{6a} and ν_{6b}.....…..... 28

Figure 3.2 ν_{9a}, ν_{15}, and ν_3..... 30

Figure 3.3 ν_1 and the Fermi resonance of $\nu_{10b} + \nu_{16b}$..……..…..... 32

Figure 3.4 Pure pyrimidine SERS spectrum with 3 Lorentzian functions.……..... 33

Table 3.3 Lorentzian functions of ν_1……...……..... 33

Figure 3.5 1M pyrimidine SERS spectrum with Lorentzian functions.……... 35

Figure 3.6 Pyrimidine-methanol SERS spectrum with 3 Lorentzian functions.…....…. 36

Figure 3.7 Evolution of ν_{8a} and ν_{8b} analyzed with Raman and SERS spectra....……..… 37

Table 3.3 Vibrational shifts of normal modes of pyrimidine…….……..… 39

Figure 3.8 Optimized molecular clusters…..…… 40

Chapter 1: Spectroscopic Methods

1.1 Spectroscopy Overview

By definition, spectroscopy is the study of interactions between light and matter. Light as an electromagnetic wave can have different effects on matter depending on the properties of the propagating wave. The spectrum illustrating these effects gives information about the fundamental chemical and physical properties of the system of study.

1.1.1 Electromagnetic Radiation

Light is a wave with oscillating perpendicular electric and magnetic fields. During the nineteenth century, light was firmly known by its wave nature; however, by the turn of the twentieth century, light was described as having qualities of a particle as well. This wave-particle duality of electromagnetic radiation is described by Equation 1.1 and Equation 1.2. The first equation mathematically definies the energy of a photon as guided by an electromagnetic wave; in other words, a wave acts as a particle.

$$E = h\nu = \frac{hc}{\lambda} \tag{1.1}$$

In Equation 1.1, h is defined as Planks constant $6.62626 \cdot 10^{-26}$ Js, ν is the frequency in Hertz, c is the speed of light $3.00 \cdot 10^{8}$ m/s, and λ is the wavelength of the light.

$$\lambda = \frac{h}{p} \tag{1.2}$$

Electromagnetic radiation can also be described as particles having wavelike properties as defined by de Broglie in 1924. He postulated that particles have the wavelength that relates the momentum of the light as defined by Equation 1.2. The momentum of the particle is found by the product of its mass and velocity. The de Broglie relation was later confirmed in 1927 by a classical diffraction experiment; this experiment was imperative in verifying the wave behavior of photons.

By understanding the physical characteristics of light propagating as both a wave and a particle, it is possible to use electromagnetic radiation to analyze the energy levels of a molecule. When light interacts with a system, three possible processes can change the energy of a given system from E_0 to E_1: absorption, stimulated emission, and spontaneous emission. Absorption of radiation results in a transition from the ground state to an excited state; stimulated emission results from a photon driving the system to transition from an excited state to the ground state; lastly, spontaneous emission of a photon occurs when a system in an excited state spontaneously transitions to the ground state. The rates of these three processes are denoted with the Einstein coefficients B_{12}, B_{21}, and A_{21} respectively. Figure 1.1 illustrates these three processes.

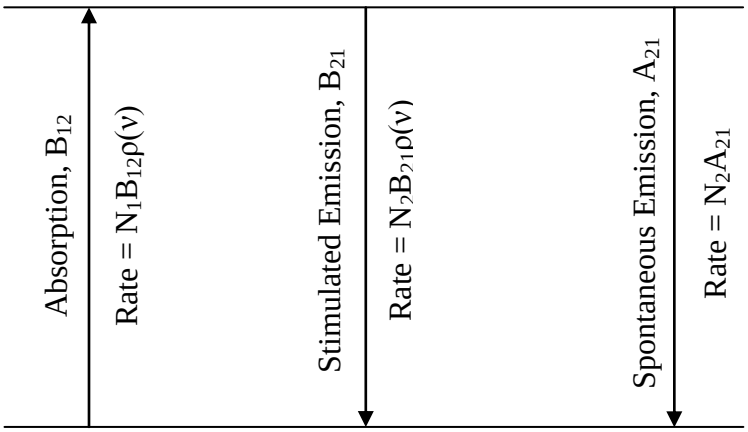

Figure 1.1 Einstein coefficients for absorption and emission.

For a system in equilibrium, the rate of transition from state 1 to 2 must equate to the transitions from 2 to 1. In other words, absorption must equal the sum of all emissions both stimulated and spontaneous. Now as can been seen from the rate equations in Figure 1.1, absorption and stimulated emission are both directly proportional to ρ(ν), the spectral density as a function of frequency. The three rates are also directly proportional to the number of molecules in the originating state referencing N_1 for absorption and N_2 for both emissions. From these observations, Einstein postulated that the ratio of spontaneous emission to stimulated emission is proportional to the cubic frequency as shown in Equation 1.3. From this equation it can be postulated that this ratio is a strong function of frequency; therefore, as frequency increases, the rate of spontaneous emission increases which competes with the stimulated emission process.

$$\frac{A_{21}}{B_{21}} = \frac{8\pi h\nu^3}{c^3} \tag{1.3}$$

This ratio was a very important concept when designing the light sources used for various experimentation measurements. A stimulated photon as a result of stimulated emission expresses the same properties of the incident radiation; therefore, the emission is collimated and coherent. Spontaneous emissions are random so it is more favorable to keep the ratio of Equation 1.3 fairly low so to maintain more stimulated emissions than spontaneous.

It is also important to have an understanding of the population of both states N_1 and N_2. The population of the lower and upper states, N_1 and N_2 respectively, are related by the Boltzmann distribution shown in Equation 1.4. Here, $h\nu = E_2 - E_1$, the energy difference between the excited and the ground state, and k is the Boltzmann constant

$1.381 \cdot 10^{-23}$ J/K. This equation expresses the equilibrium between nondegenerative energy levels.[1-3]

$$\frac{N_1}{N_0} = e^{-h\nu/kT} \tag{1.4}$$

1.1.2 Quantum Mechanics

In order to describe the interactions between electromagnetic radiation and matter, the many energy levels of molecules can be mathematically determined with use of the time-independent Schrödinger equation. In Equation 1.5, $\hat{H}$ is the Hamiltonian or the total energy operator of the system. The wavefunction, ψ, describes the state of a particle in three dimensions, and the quantum numbers, subscript n, represent the quantum numbers of allowed states for the system for different energies, E.

$$\hat{H}\psi_n = E\psi_n \tag{1.5}$$

Spectroscopy is the method used to probe these different energies. Light following the stipulation outlined in the Bohr frequency condition, Equation 1.6, can induce a transition from a lower to an upper energy state, E_1 to E_2 respectively.

$$\nu = \frac{E_2 - E_1}{h} \tag{1.6}$$

According to this equation, the frequency of the incident radiation must equal that of the energy needed for a transition to occur from state 1 to 2. In order to calculate the physical properties of a molecule as opposed to only solving for the total energy as outlined in Equation 1.5, a more general form of the Schrödinger equation may be applied with the physical property operator, $\hat{A}$, with eigenvalue a_n.

$$\hat{A}\psi_n = a_n\psi_n \tag{1.7}$$

However, the conditions set by this eigenvalue equation are not always met if the system is in a different state than the product of the eigenvalue constant and the wavefunction; therefore, the expectation value must be calculated in which <A> represents the average physical property.

$$<A> = \int \psi_m^* \hat{A} \psi_n \, d\tau \tag{1.8}$$

The expectation value may be used to calculate the change between states *m* and *n* of a system. This integral is used for many operators such as the position, momentum, or, as will be covered later in this paper, the transition dipole integral. These quantum mechanical equations and principles are applied to different spectroscopic studies in order to determine the energies of the various energy levels being probed.[1-3]

1.2 Vibrational Spectroscopy

Vibrational spectroscopy is a type of spectroscopy that probes the vibrational motions of molecules usually with the absorption of the infrared region of the electromagnetic spectrum. A vibrational spectrum of a molecule can give insight into the molecular structure of a molecule as well as possible interactions in bulk solution. As described in the previous section, incident radiation of energy matching that of the energy needed to excite an electron from one level to one of a higher energy can cause a transition; more specifically, the energy provided by infrared radiation causes vibrational transitions within a molecule. The various transitions that could occur as a result of different energies of incident electromagnetic radiation are illustrated in Figure 1.2.

By applying the Boltzmann distribution (Equation 1.4) it can be determined that the population of the ground vibrational state is much higher as compared to the

population of the first excited state. Generally with vibrational spectroscopy, the only observable transition is from the ground state to the first excited vibrational state. Selection rules govern transitions that could occur between states. The general selection rule for vibrational spectroscopy used to calculate the probability of a given transition is denoted the transition dipole integral in Equation 1.9.

$$\mu_x^{mn} = \int \psi_m^*(x)\mu_x(x)\psi_n(x)\, dx \neq 0 \tag{1.9}$$

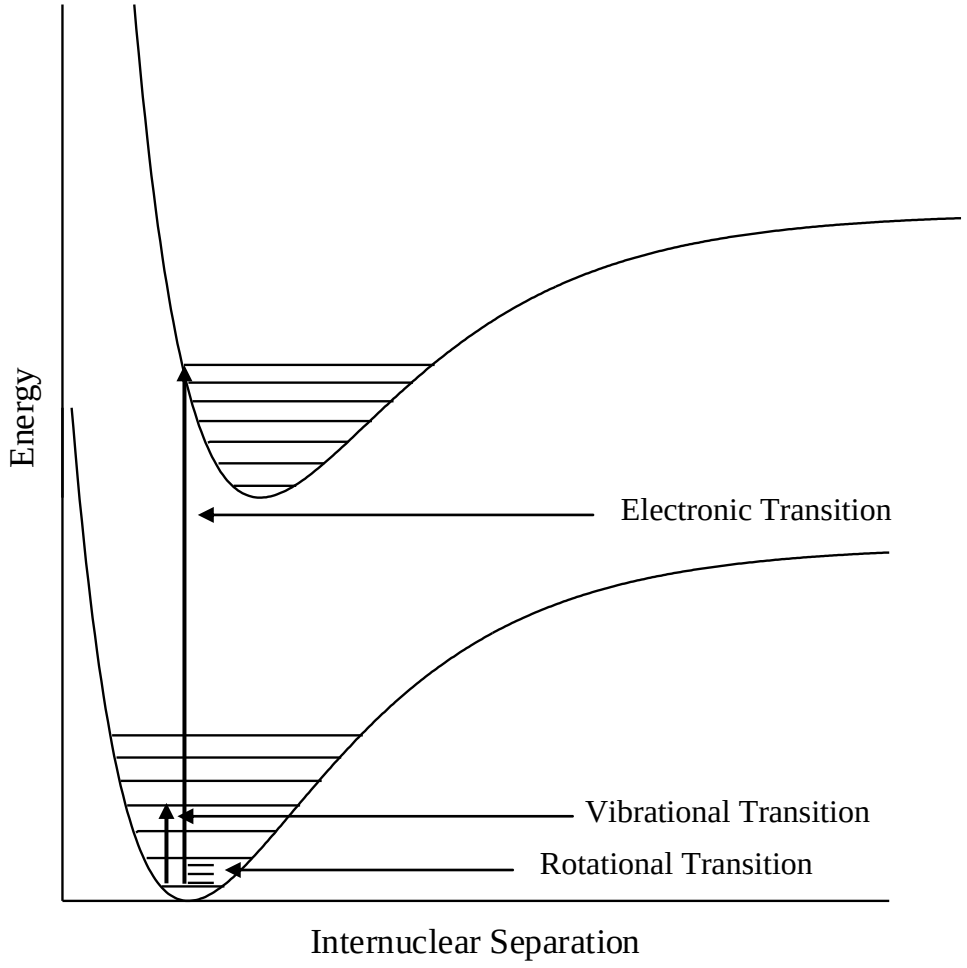

Figure 1.2 Possible transitions caused by electromagnetic radiation.

The dipole moment along the electric field, μ_x(x), determines how the molecule will interact with the incident radiation. The transition dipole integral must be nonzero from state *m* to *n* in order to denote a transition.

To physically describe these transitions, a coordinate system must be defined; the vibrations can therefore be described by the change in coordinates of atoms within a molecule. A nonlinear molecule of N atoms has 3N-6 normal vibrational modes while a linear molecule has 3N-5 normal vibrational modes. Normal refers to the displacement of an atom is orthogonal for any two modes. The 3N corresponds to the three degrees of freedom of motion in a three coordinate system. The 6 denotes the three translational and three rotational motions observed for a molecule; therefore, the number of vibrational motions equates to the total molecular motions minus the translational and rotational motions. A linear molecule only displays two rotational motions since the rotation about its molecular axis cannot be observed; the one less rotational motion for linear molecules is observed for the subtraction of 5 for the translational and rotational motions.

Each of these normal modes has an associated energy that is denoted as a peak on a spectrum. However, more than one mode may have the same energy associated with the molecular motions; these energies are designated as degenerate. These spectral peaks, therefore, can give information as to the molecular motions of a given system.[1-3]

1.3 Raman Spectroscopy

Raman spectroscopy is a method also used to study the vibrational as well as rotational motions of molecules. This means of experimentation utilizes a monochromatic light source, generally a laser, to irradiate a sample and excite the molecule to a virtual energy

state. When the molecule relaxes from this virtual state, the photon becomes scattered at either the same frequency as the incident radiation, denoted Raleigh (elastic) scattering, or it is scattered at some shifted frequency, Raman (inelastic) scattering. The first recognition of the scattering of photons having a different frequency than that of the incident radiation was made by C.V. Raman in 1928. Raman utilized the sun for a radiation source; however, in current years with the advancement in technology, lasers are generally used.[1-4]

Raman scattering occurs when the molecule excited to a virtual state returns to a state either at a higher or a lower energy level than the beginning state. Stokes scattering is defined as the relaxation from a virtual state to a level of greater energy than that of the initial state; this process results in a scattered photon of less energy and larger wavelength than that of the incident radiation. The other type of Raman scattering, anti-Stokes scattering, is defined when relaxation from the virtual state to a level of lower energy than that of the initial state occurs resulting in a scattered photon of greater energy and smaller wavelength than the incident radiation. The frequency of the scattered photon resulting from the Raman effect, therefore, is not of the same frequency of the incident radiation; the difference in these energies equates to the frequency of the molecular vibration. The energy shifts are characteristics of the different vibrations within a molecule and can therefore be used to characterize a system.[1-3,5,6] A schematic of scattering effects is illustrated in Figure 1.3 on the following page.

An applied electric field can induce a dipole moment in a molecule. This induced dipole is linearly proportional to the product of the polarizability of the molecule and the energy of the applied electric field. This relation is shown in Equation 1.10 in which α is

a constant. A change in the polarizability of a molecule is required for a mode to be considered Raman active. Distortion of the electron cloud leads to changes in the dipole moment; therefore, the transition dipole integral (Equation 1.9) is nonzero denoting that there is a probable transition The polarizability changes of a molecule are dependent on the direction of the electric field.[1-3,6]

$$\mu_{ind} = \alpha E_0 \cos\omega t \qquad (1.10)$$

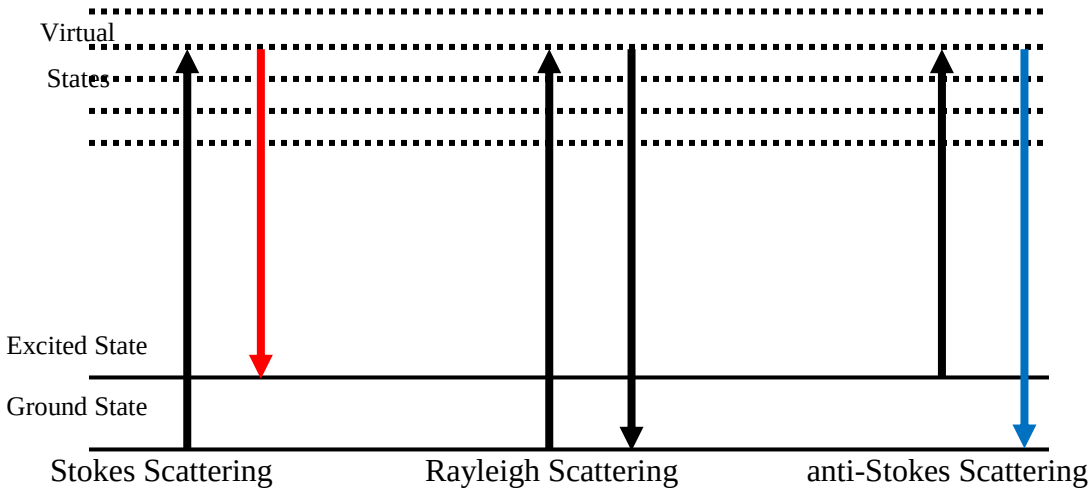

Figure 1.3 Schematic of Rayleigh and Raman scattering.

According to classical theory, the applied electric field induces the dipole moment by the electrons and nuclei moving in opposite directions as a response. The applied electric field itself is of a known wavelength that is much larger than the molecular dimensions of the compound of study. This electric field, as described by Equation 1.11, induces an oscillating dipole moment.

$$E = E_0 \cos(\omega t) \qquad (1.11)$$

Since the vibrations are causing a change in the electron density of the molecule, the polarizability constant of Equation 1.10 must be considered as a constant as well as and oscillating term. The polarizability is now expressed a sum of the static term and oscillating term in Equation 1.12. Here, the second term denotes a change in polarizability for a given vibrational mode, Q_i.

$$\alpha = \alpha_0 + \frac{\partial \alpha}{\partial Q_i} Q_i \cos(\omega t) \tag{1.12}$$

Therefore, according to Equation 1.12, if the polarizability does not change with a given vibration, then that vibrational mode is not considered Raman active. From the classical model, the induced dipole moment can oscillate at other frequencies than the frequency of the incident radiation, ω_I. This phenomenon is caused by the oscillating polarizability. Therefore, by combining Equations 1.11 and 1.12 taking the incident and induced dipole moment frequencies, Equation 1.13 can be written.

$$\mu_{ind} = \alpha_0 E_0 \cos\omega_I t + \frac{\partial \alpha}{\partial Q_i} Q_i E_0 \cos\omega_I t \cos\omega t \tag{1.13}$$

Equation 1.13 can be further simplified using a known trigonometric identity. The equation for Raman scattering as described by classical theory is described by Equation 1.14.

$$\mu_{ind} = \alpha_0 E_0 \cos(\omega_I t) + \frac{1}{2}\frac{\partial \alpha}{\partial Q_i} Q_i E_0 \{\cos[(\omega_I + \omega)t] + \cos[(\omega_I - \omega)t]\} \tag{1.14}$$

The first term of Equation 1.14 refers to the scattering at the same frequency as the incident radiation, therefore, corresponding to Rayleigh scattering. In the second term there are 2 frequencies represented, one of $\omega_I + \omega$ and $\omega_I - \omega$ which correspond to the anti-Stokes and Stokes scattering respectively.[2]

Photons will only experience Raman scattering for only approximately 1 photon in a million. This low probability of scattered photons is even lower when subdivided into anti-Stokes and Stokes scattering with Stokes scattering being the photons usually detected in Raman spectroscopy.[6] Because of this low probability, and even lower probability for observing Stokes scattering, it is advantageous to enhance the Raman signal.

1.4 Surface Enhanced Raman Spectroscopy

Surface enhanced Raman spectroscopy (SERS) is a Raman spectroscopy enhancing technique that utilizes an active metal substrate on the surface of a glass cover slide for adsorbing a molecule. As with Raman spectroscopy, a strong laser source is used for SERS. The interaction of this laser with the metal substrate produces plasmon resonances. These plasmon resonances are then responsible for the enhancement of signal of several orders of magnitude.

The metal used as substrate must provide a large enhancement. The SERS enhancements are strongly wavelength dependent since because of the reliance on plasmon resonances. Most of the metals, therefore, only exhibit a strong SERS enhancement in a small wavelength range. The two most commonly used metals are gold and silver operate in the region of 400-1000 nm. Copper and platinum have also been studied as SERS substrates, but they do not create the large enhancements seen with gold and silver. The metal must also have dimensions less than that of the wavelength range, and a rough surface is preferred over a smooth surface.

The metals used for the active metal substrate must contain free conduction electrons. Plasma is formed by the metal's free electrons moving around fixed positive ions. It is the optical properties of this plasma that provide the characteristic optical properties of the metal substrates. A plasmon is the quantum quasi-particle in a plasma charge density. When the incident radiation comes in contact with the metal, electrons of the metal are excited resulting in the desired optical properties of the substrate. This interaction between the incident radiation and the metal substrate is known as the electromagnetic enhancement. There is, however, another means of enhancement that occurs from the interactions of the metal substrate with the adsorbate. Though this chemical enhancement is not of the same magnitude as the electromagnetic enhancement, it is still of importance especially within the analysis of the SERS spectra reported in this thesis.

The chemical enhancement is not actually related to the SERS effect; instead it is considered a characteristic of the adsorbate and its interactions with the metal substrate. This interaction with the metal changes the nature of the adsorbate which causes variations in the SERS spectrum. The chemical effect can be considered as an enhancement though since it is multiplicative of the electromagnetic effect.

One type of chemical enhancement that has been studied most extensively is the mechanisms of charge transfer. Three types of charge transfer are possible. First, if the adsorbate is not covalently bound to the metal, the metal may perturb the electron density of the adsorbate. The change in electron density causes a change in polarizability which can therefore be detected by the Raman effect but at a different frequency than predicted normal mode. A second type of charge transfer occurs when the adsorbate is bound to the

metal causing a change in the polarizability of the molecule of study. The last mechanism is more complex than the two just mentioned. In the third charge transfer mechanism, if the difference of the HOMO or LUMO energies as well as the Fermi level of the metal match that of the incident radiation.[7]

Chapter 2: Pyrimidine

Diazines are a class of 6-membered heterocyclic molecules that contain 2 nitrogen atoms of sp^2 hybridization in the ring. These water-soluble colorless compounds encompass the three molecules pyridazine (1,2-Diazine), pyrazine (1,4-Diazine), and pyrimidine (1,3-Diazine).[8,9] These three molecules are illustrated in Figure 2.1 below.

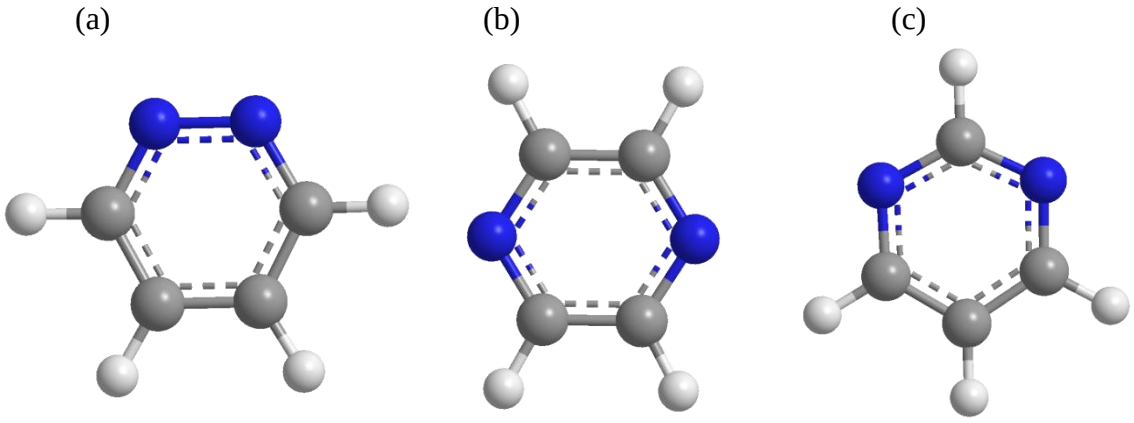

Figure 2.1 The three diazines molecules (a) pyridazine, (b) pyrazine, and (c) pyrimidine.

Pyrimidine is a biological, naturally occurring diazine of most significance since it is of great prevalence in the compounds composing our genetic makeup.[9] It first became a molecule of chemical development in 1883 and catalyzed a new study of synthetic chemistry all involving this heterocyclic nitrogenous compound. It was within the following decade that pyrimidine derivatives were being synthesized. In 1893, it was discovered that the nucleic acids thymine and cytosine contain pyrimidine as the parent compound; it was not until a few years later that uracil was discovered to be a pyrimidine

derivative. The successive years led many to many synthetic mechanisms to produce pyrimidine derivatives that now have wide biological and medicinal implications.[10]

2.1 Biological Importance

Pyrimidine derivatives are of great biological and medicinal significance. As previously mentioned, pyrimidine is present in the naturally occurring nucleic acids thymine, cytosine, and uracil; thymine and cytosine are the biological building blocks for deoxyribonucleic acid (DNA) while cytosine and uracil are the fundamental units for ribonucleic acid (RNA). Other naturally occurring pyrimidine derivatives include a number of vitamins: folic acid, riboflavin, thiamine, and barbituric acid.[9,11] Figure 2.2 illustrates the molecular structure of these naturally occurring biologically important pyrimidine derivatives. Folic acid plays an important role in red blood cell (RBC) maturation as well as DNA synthesis.[12] Riboflavin holds an important role in the body involving redox reactions for the production of FAD, an important compound in energy production; riboflavin enzymes also are an important component in the breakdown of drugs and nutrients.[13] Thiamine, otherwise known as Vitamin B_1, is found in many types of grains such as yeast, rice, and cereal; a thiamine deficiency, denoted beriberi, results in nervous system damage.[2] Lastly, barbituric acid is presently used for sedatives.[9,11]

Pyrimidine derivatives also are prevalent in many pharmaceutical products involving antibiotics as well as compounds with antibacterial and anticancer characteristics. One such antibiotic is 5-hydroxymethyl-2-methoxypyrimidin-4-amine, otherwise known as bacimethrin which is known for its defenses against *Staphylococcal aureus* (staph infection). Trimethoprim is a known antibacterial drug that contains

pyrimidine; this compound is responsible for the selective inhibition of a class of bacterial enzymes called dihydrofolate reductase (DHFR).

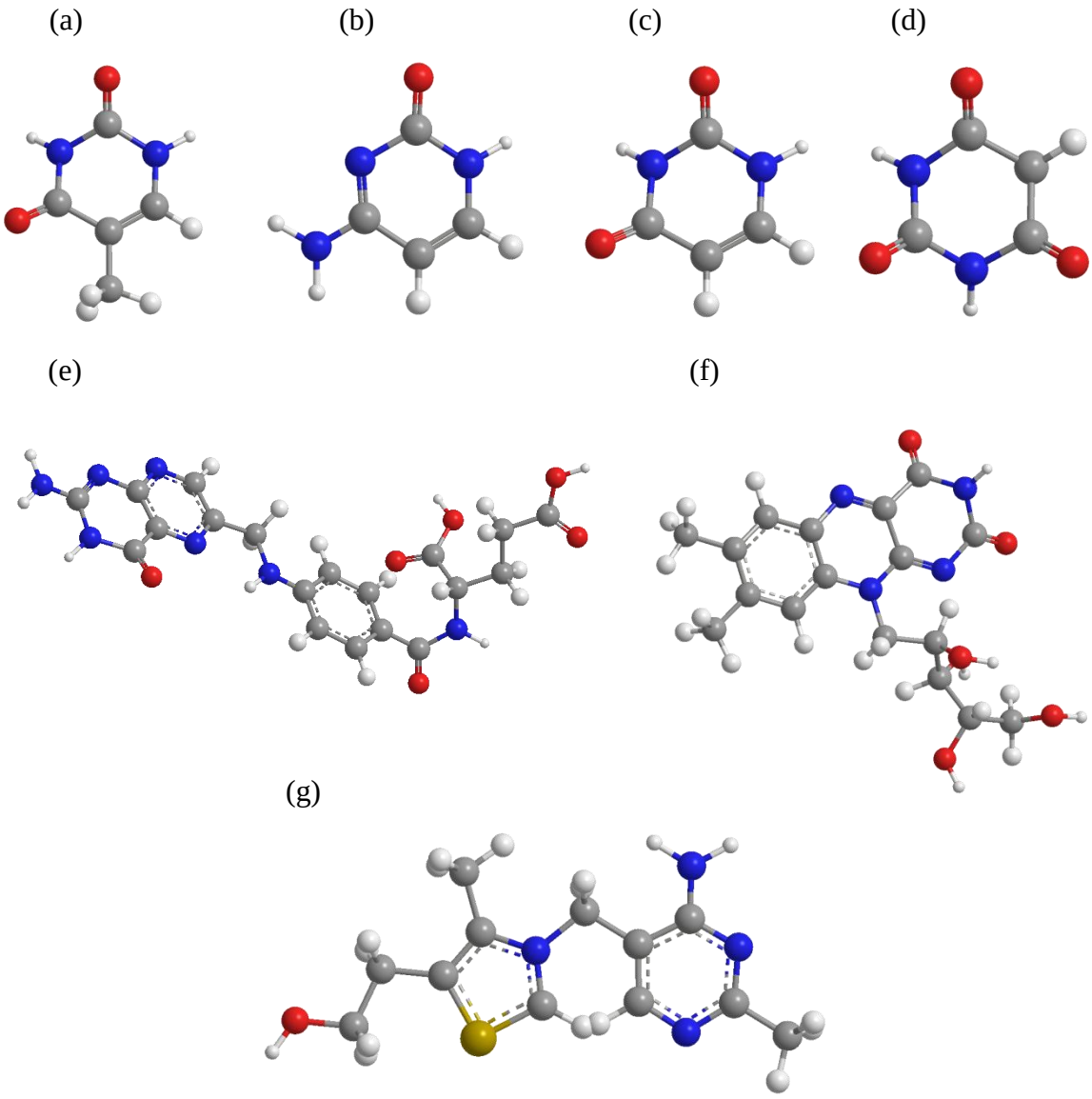

Figure 2.2 Naturally occurring pyrimidine derivates prevalent in biological systems (a) Thymine (b) Cytosine (c) Uracil (d) Barbituric Acid (e) Folic Acid (f) Riboflavin (g) Thiamine.

Pyrimidine derivative also have a presence in anticancer products. One such compound is 1-*β*-*D*-Arabinosylcytosine; this compound also is used in therapies for the herpes virus.[11] Pyrimidine and its derivatives are a very large part of biologically relevant molecules and understanding its role within the body as well as the possible interactions within the body can help fuel medicinal research of drugs containing pyrimidine derivatives.

2.2 Previous Studies

Four previous studies will be outlined in this chapter. These publications report vibrational modes of pyrimidine or pyrimidine solvated systems by experimental spectroscopic means or computations data. Results reported by Austin A. Howard elucidated the blue-shifted normal modes of pyrimidine when in a water-solvated system; this publication utilized both experimental and computational results to make the reported conclusions.[14] The next study by J. Coleman Howard further explored the hydrogen bonded networks formed between water and pyrimidine. Howard utilized DFT computations to characterize pyrimidine-water clusters with 1 to 7 water molecules.[15] Ashley M. Wright presented results of the normal modes of crystalline pyrimidine as compared to the normal modes of liquid pyrimidine; these modes were also compared to DFT calculations to assign the vibrational motions.[16] Lastly, a previous study on the research by Centeno et al. outlines a charge transfer mechanism between pyrimidine and the silver metal substrate used for SERS.[17] These four previous studies were useful in for the development of the research presented in this honors thesis. A synopsis of these studies is the remainder of this section.

2.2.1 Hydrogen Bonding Effects on Pyrimidine

A previous study led by Austin A. Howard analyzed 10 normal modes of pyrimidine by means of Raman spectroscopy and density functional theory (DFT) calculations in order to present the effects of hydrogen bonding with the pyrimidine. Experimentally, an excitation source of an Ar^+ laser with 514.5 nm line was utilized for the study; the same excitation source is used for the study outlined later in this paper. Howard et al. obtained spectra of 6 different concentrations of pyrimidine/water mixtures including pure pyrimidine and the 5 following diluted concentrations of χ_{H2O}: 0.15, 0.30, 0.50, 0.70, and 0.90. It was concluded that all 10 normal modes studied blue-shifted to higher energies with the pyrimidine water-solvated system; however, these shifts were all of different magnitudes and increased with increasing mole fractions of water. The reported experimental shifts of a select 7 of the reported 10 normal modes are listed in Table 2.1.[14] The current research reported in this honors thesis proved Howard's results true as well as expanded the study to include the SERS spectra of pyrimidine and pyrimidine water mixtures.

Mode	Pure Pyrimidine	1 M Pyrimidine
ν_{6b}	626	639
ν_{6a}	681	686
ν_1	990	1004
ν_{9a}	1139	1144
ν_3	1228	1231
ν_{8a}	1564	1570
ν_{8b}	1571	1583

Table 2.1 Normal modes of pyrimidine and pyrimidine/water mixture.[14]

2.2.2 Micro-Hydrated Pyrimidine Structures

The goal of the work by Howard et al. in 2011 was to expand on the current computational information of pyrimidine/water mixtures. These mixtures are denoted PyW_n with the subscript *n* representing the number of water molecules present around the pyrimidine. DFT calculations were utilized to determine the most stable hydrogen bonded networks of the PyW_n as well as model the vibrational shifts of pyrimidine/water mixtures to more accurately characterize the concentration dependence previously reported by A. Howard et al. Many PyW_n were reported including structures of 1 to 7 waters. It was concluded that the lowest energy structures of $n \geq 4$ included preferential binding of water molecules on one side of the pyrimidine molecule; these water molecules formed a cluster with one of the waters hydrogen bonding to one of the two nitrogen atoms present on the pyrimidine. It was also reported, however, that this preferential bonding to one side of the pyrimidine is not supported by experimental data. The shifts in vibrational frequencies observed experimentally more closely agree with the computational data of water clusters hydrogen bonding to both of the nitrogen atoms on the pyrimidine molecule as opposed to just one.[15]

2.2.3 Normal Modes of Crystalline Pyrimidine

The vibrational normal modes of crystalline pyrimidine were studied in 2011 by Ashley M. Wright et al. using Raman spectroscopy and DFT calculations. These experimental and computational results were also compared to the normal modes of liquid pyrimidine. Wright et al. published results comparing the shifts of normal modes of liquid pyrimidine to the crystalline pyrimidine. Overall agreement between experiment and theory was

reported with the greatest effect on modes involving those with motions of hydrogen atoms. Table 2.2 lists the normal modes of both liquid and crystalline pyrimidine reported.

Of the normal modes listed in Table 2.2, ν_{8a} is characterized by motions of hydrogen atoms. When comparing the liquid pyrimidine spectrum to the crystalline pyrimidine spectrum, ν_{8a} experienced a split which is indicative of strong interactions involving the hydrogen atoms of this normal mode. Overall, though, there is a general trend of blue-shifting of the normal modes when going from liquid to solid pyrimidine. It was reported by Wright et al. that this phenomenon is caused by anharmonicity changing the force constant.[16]

Mode	Liquid Pyrimidine	Crystalline Pyrimidine
ν_{6b}	626	628
ν_{6a}	681	680
ν_1	990	992
ν_{9a}	1139	1142
ν_3	1228	1242
ν_{8a}	1564	1568
ν_{8b}	1571	1577

Table 2.2 Normal modes of liquid and crystalline pyrimidine.[16]

2.2.4 Charge Transfer Mechanism of SERS

In 2006, Silvia P. Centeno et al. studied the charge transfer states of pyrimidine bonded to silver nanoclusters utilizing SERS. It has been noted previously the chemical enhancement of SERS is of lesser contribution than that of the electromagnetic

enhancement. It was the goal of the study to develop a method to quantitate the chemical enhancement, otherwise known as the charge transfer (CT), contribution to a SERS spectrum. They postulated a two step process for the CT mechanism in which a laser photon induces the transfer of an electron from the silver metal nanoclusters to an empty orbital of the adsorbate; this electron transfer results in a CT state. The second step of this mechanism results from the transferred electron returning to the metal along with the emission of a scattered Raman photon from the molecule.

Experimentally, Centeno et al. studied the Raman spectrum of pyrimidine and a 1 M pyrimidine solution and the SERS spectrum of 1 M pyrimidine at varying silver electrode potentials in order to deduce any effects of CT. Table 2.3 below is an excerpt of the vibrational frequencies found experimentally by means of Raman and SERS spectroscopy. The results of their experimentation were compared with computational data in order to confirm results. They speculate that the charge transfer occurring between the silver metal substrate and the adsorbate is the source of the excited levels.[17]

Mode	Raman (cm^{-1})		SERS (cm^{-1}) -0.5 V
	Pure Pyrimidine	1 M Pyrimidine	1 M Pyrimidine
ν_{6b}	624	638	636
ν_{6a}	680	684	682
ν_{1}	993	1007	1007
ν_{9a}	1140	1146	1140
ν_{3}	1231	1233	1233
ν_{8a}	1568	1574	1564
ν_{8b}	1576	1588	1584

Table 2.3 Vibrational frequencies of pyrimidine and pyrimidine solution.[17]

The validity of these conclusions can be somewhat skeptical though. In this publication, pure pyrimidine and 1 M pyrimidine Raman as well as aqueous pyrimidine SERS were studied in an attempt to separate the charge transfer effects. Considering that the charge transfer occurs from the transfer between metal substrate and adsorbate, to accurately deduce charge transfer effects pure pyrimidine SERS would need to have been analyzed. By using the experimental procedures outlined in this paper, it would be difficult to separate the means of charge transfer when the only SERS spectra has another molecule present than just the adsorbate and metal substrate.

Chapter 3: Vibrational Spectroscopy of Pyrimidine and Pyrimidine Mixtures to Analyze Charge Transfer Induced Shifts

3.1 Introduction

Since the discovery of surface enhanced Raman spectroscopy (SERS) nearly 35 years ago, much research has been accomplished with the majority of its recognition being in the more recent years.[18-24] SERS is having a great influence on the detection of various molecules of biological importance. Recently SERS has been utilized for the purpose of single molecule detection, nanoparticle probes, and for use as a biosensor. Even certain biocompatible dyes have been determined to exhibit SERS activity and can bind themselves to various biological macromolecules to resolve the macromolecule in a bulk solution.[20, 25-30] By using this means of vibrational spectroscopy to study organic molecules, the changes in spectra denote interacting atoms, either solute-solute or metal-solute, and can illustrate the effect of bond changes within the molecular structures.[31-33]

Organic molecules essentially compose all biological macromolecules including those of protein and nucleic acid components. The majority of these macromolecules incorporate one or more nitrogen atoms in the molecular structure.[34] Considering this importance of nitrogen in biological molecules, pyridine and pyrimidine have been a topic of study given that they are both heterocyclic organic compounds containing

nitrogen atoms.[35] Pyridine has one nitrogen atom while pyrimidine contains two nitrogen atoms at positions one and three. The nitrogen atom of these biological species generally contains a lone pair of electrons because of the delocalized nature of the heterocycles. Therefore, the nitrogen atom is ideal for interacting with other atoms and molecules.[34] In aqueous solutions, the nitrogen interacts with the water molecules by the formation of hydrogen bonds, and during SERS analysis, the nitrogen can interact with the silver SERS substrate producing electromagnetic and chemical enhancements. Pyridine was first used with SERS because it proved to be a good analyte considering it only has one nitrogen atom in its structure available for interactions with the SERS substrate or solvent of various solutions.[36-38] The vibrational modes of pyrimidine are now being analyzed using Raman and SERS spectroscopy because of the presence of two nitrogen atoms in its structure.

Here, I present the effect of silver on pyrimidine molecules as well as the competition for charge transfer among pyrimidine, solvent, and silver substrate. The nitrogen atoms of the pyrimidine molecule allow for hydrogen bonding with water when in aqueous solution; however, with the SERS chemical effect adding the factor of interactions with the silver metal substrate, the pyrimidine molecule may form hydrogen bonds with water as well as temporarily interact with the metal substrate causing frequency shifts depending on the particular vibrational normal mode. The aim of this study is to separate the effects of the hydrogen bonding with solvent from the silver interactions with pyrimidine and like molecules as well as to show how different solvents affect the magnitude of charge transfer.

3.2 Experimental Procedures

In a Raman spectroscopy experimental setting, a strong excitation source must be used since the Raman scattering is much weaker than the Rayleigh scattering. For the purposes of the research presented in this thesis, the 514.5 nm line of a Coherent Innova 200 Ar^+ laser was used. This same excitation source was used for obtaining all spectra, both Raman and SERS. Since the various spectra were acquired on different occasions, a means of calibrating the laser was needed in order to have accurate spectra. 99.6% assay Naphthalene (EMD Chemicals) was used for this purpose. This compound has vibrational modes across the region of interest enabling an accurate calibration of the full spectrum. A 514.5 nm laser line filter was placed in front of the sample to attenuate background wavelengths from the laser as well as to block the majority of any ambient lighting. A half-wave plate (Thorlabs) was also placed in front of the sample in order to rotate the polarization of the laser from horizontal to vertical. Laser powers ranging from 3 mW to 30 mW were used to obtain spectra; no spectral features changed with the changing power so all spectra presented are excited using 15 mW of power. The 300 mm, 1200 mm, and 2400 mm gratings of an Acton SP2500 0.500m Imaging Triple Grating Monochromator/Spectrograph by Princeton Instruments and a Princeton Instruments ProEM 1024 CCD camera were utilized to detect all spectra. Raman spectra were accumulated with a 60 second exposure time while SERS spectra were obtained using 0.5-2 second exposure time.

Commercially obtained 99% assay pyrimidine (Sigma-Aldrich) was used with no further purification. Nanopure water from a Barnstead Nanopure Diamond ultrapure water system and 99.93% biotechnology grade methanol (Sigma-Aldrich) were used to

make the diluted solutions of pyrimidine with mole fractions of χ_{H2O}= 0.982 and χ_{MeOH}=0.983. The solutions were placed in a sonicator for 30 seconds before every spectral acquisition to ensure homogeneity of the solution.

The Raman spectra were obtained by pipetting the pyrimidine or pyrimidine solution on a cover slide; however, with SERS, organic molecules and contaminants in the air can become a serious problem and set back. For means of obtaining SERS spectra, the glass slides had to be properly cleaned and preserved so that a minimal amount of contaminant could adhere to the surface. Glass cover slips were cleaned in a piranha solution of a 3:1 ratio of sulfuric acid to hydrogen peroxide for 15 minutes and subsequently washed twice in distilled water for 10 minutes each time, refreshing the water after the first wash. Washing the slides in a piranha solution ensures that all organic matter has been removed from the cover slip. By ridding of all contaminants before the deposition of silver, the SERS spectra would contain less exogenous peaks from foreign matter. An AUTO 306 Vacuum Coater with Diffusion Pumping System (Edwards High Vacuum International) was used for depositing 5 nm of silver at a rate of 1-2 Å/s on the piranha cleaned slides. 99.99% metal basis silver wire with a 1.0 mm diameter (Sigma-Aldrich) was used for this deposition. The slides were left under vacuum for at least 30 minutes or until use to ensure minimal contamination.

3.3 Results and Discussion

The full spectrum is divided into four regions to simplify the visualization of the spectroscopic effects. The SERS effect is employed to enhance the Raman signal for better interpretation of the interactions among pyrimidine molecules, pyrimidine-water

interactions, and pyrimidine-methanol interactions. The SERS effect is also used to deduce possible interactions between pyrimidine and silver molecules as the controversial inherent chemical enhancement of this experimental method. The normal modes and experimental shifts from the pyrimidine Raman spectra are listed in Table 3.1 and 3.2, respectively. These tables include the whole spectral region studied and will be referred to throughout this thesis.

Mode	pyr	pyr-water	pyr-MeOH	pyr-Ag	pyr-water-Ag	pyr-MeOH-Ag
ν_{6b}	624	637	631	627	-	635
ν_{6a}	679	683	682	680	-	682
ν_{1}	990	1005	996	1002	1003	1002
ν_{10b}	1052	1056	1054	1053	1054	1055
ν_{16b}	1072	1073	1073	1070	1070	1071
ν_{9a}	1139	1144	1142	1138	1140	1140
ν_{15}	1160	1168	1164	1172	1173	1174
ν_{3}	1228	1232	1229	1234	1233	1235
ν_{8a}	1564	1570	1566	1561	1560	1561
ν_{8b}	1571	1583	1577	1581	1580	1580

Table 3.1 Raman and SERS normal modes (cm^{-1}) of pyrimidine and pyrimidine mixtures.

Mode	pyr-water	pyr-MeOH	pyr-Ag	pyr-water-Ag	pyr-MeOH-Ag
ν_{6b}	13	7	3	-	11
ν_{6a}	4	3	1	-	3
ν_{1}	15	6	12	13	12
ν_{10b}	4	2	1	2	3
ν_{16b}	1	1	-2	-2	-1
ν_{9a}	5	3	-1	1	1
ν_{15}	8	4	12	13	14
ν_{3}	4	1	6	5	7
ν_{8a}	6	2	-3	-4	-3
ν_{8b}	11	6	10	9	9

Table 3.2 Shifts from pure pyrimidine Raman modes.

3.3.1 Modes ν_{6a} and ν_{6b}

Figure 3.1 shows the spectral region with the modes ν_{6b} and ν_{6a}. These modes are the in-plane CNC/CNC bending and the in-plane CCC/NCN bending respectively. When comparing these normal modes of pyrimidine in solution with either water or methanol, a greater blue shift is observed in the pyrimidine-water mixture as opposed to the pyrimidine-methanol solution.

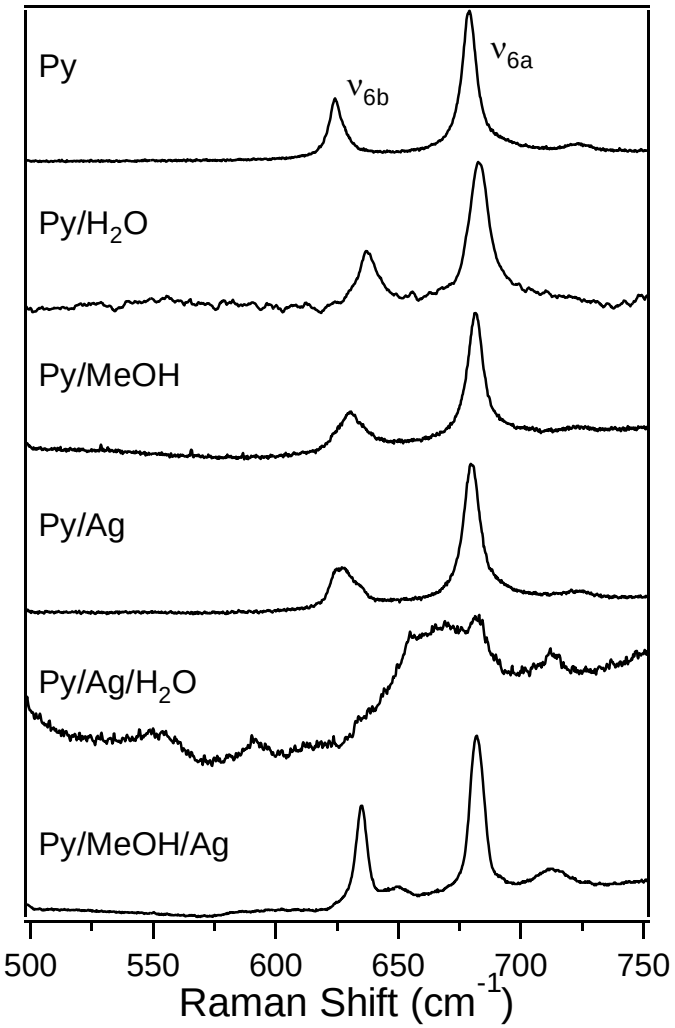

Figure 3.1 Raman and SERS spectra of the modes ν_{6b} and ν_{6a} of pyrimidine and pyrimidine mixtures.

Water is capable of forming 4 hydrogen bonds since it can donate two hydrogen atoms forming 2 different hydrogen bonds as well accept 2 hydrogen bonds on its oxygen atom forming 2 more hydrogen bonds; methanol on the other hand can only potentially form 3 hydrogen bonds donating a hydrogen for one bond and accepting two hydrogen atoms on its oxygen atom for the other two hydrogen bonds. The larger magnitude of blue shifting experienced with the pyrimidine-water mixture can be attributed to the greater number of possible intermolecular interactions in the form of hydrogen bonds with the nitrogen atoms of the pyrimidine. Though ν_{6b} and ν_{6a} experimental shifts cannot be accurately determined for the 1M aqueous pyrimidine SERS, the Raman and SERS spectral shifts of the pyrimidine-methanol solution can be compared. The hydrogen bonded networks formed between pyrimidine and methanol cause blue shifts of these two normal modes in both the Raman and SERS spectra with greater magnitude of shifting occurring in the Py/MeOH SERS spectrum with the appearance of two new modes. The greater energy shifts of the SERS spectrum may be attributed to charge transfer between the silver substrate and pyrimidine.

3.3.2 Modes ν_{9a}, ν_{15}, and ν_3

Figure 3.2 shows the Raman and SERS spectra of ν_{9a}, ν_{15}, and ν_3. An NCN bending mode, ν_{9a}, experiences a slight red shift, shift to lower energy, of -1 cm^{-1} comparing the pyrimidine-silver interactions in the SERS spectrum to that of the pyrimidine Raman spectrum; however, this mode shows a slight blue shift of +1 cm^{-1} when the pyrimidine is subject to solvent interactions as well as interactions with the silver. The vibrational shifts of ν_{9a} in the SERS spectra of pyrimidine-solvent are not as

large as the blue shifts reported for the Raman spectra of pyrimidine-water and pyrimidine-methanol. This variation can be caused by the competition of binding among pyrimidine, silver, and solvent molecules. The silver SERS substrate is most likely retarding the amount of hydrogen bonding by interacting with the pyrimidine. The opposite trend occurs with ν_{15} and ν_3 in which larger shifts occur with the SERS spectra of pyrimidine solutions compared to the Raman spectrum of the solutions. Both ν_{15} and ν_3 are in-plane CH bending modes.

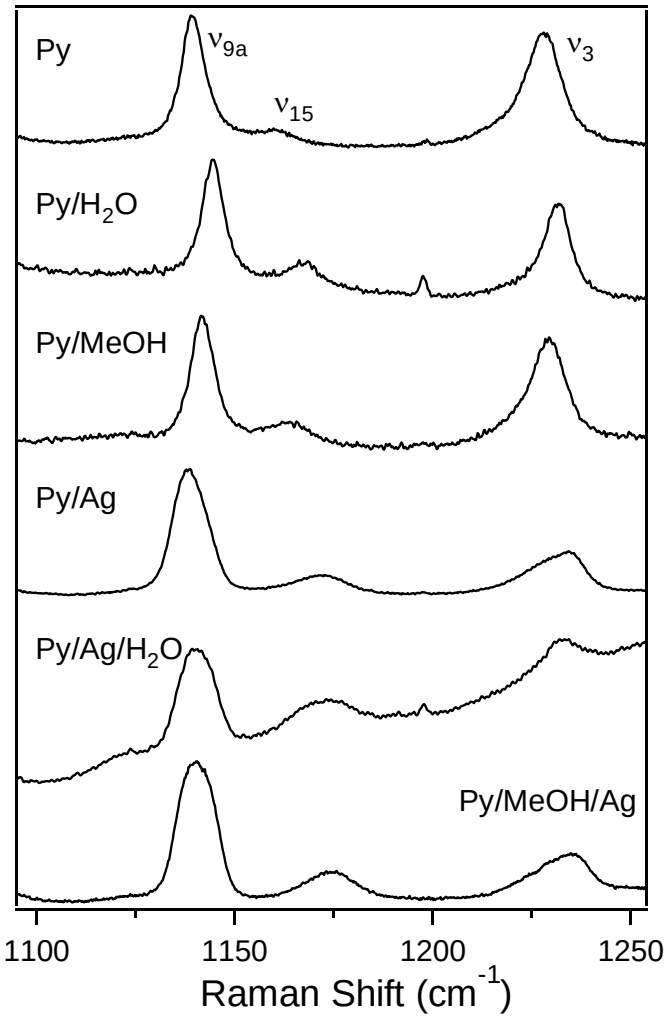

Figure 3.2 Raman and SERS spectra of the modes ν_{9a}, ν_{15}, and $\nu_{3.}$

3.3.3 Modes ν_1 and Fermi Resonance $\nu_{10b} + \nu_{16b}$

Figure 3.3 shows the spectrum for the totally symmetric mode, ν_1, and the Fermi resonance, $\nu_{10b} + \nu_{16b}$. Fermi resonances are attributed to the anharmonic mixing of 2 vibrational modes; the vibrational modes must be close in energy and have the same symmetry for mixing to occur. The result of mixing is two spectral peaks that split depending upon the original unmixed energies of the normal modes. The closer the energies, the larger the splitting. The two resulting peaks represent the originating vibrational modes; the mode of higher energy results in the Fermi resonance peak of larger energy while the mode of lower energy results in a Fermi resonance peak of lower energy. Here, the Fermi resonance results from the mixing of the 2 fundamental modes ν_{10b} and ν_{16b} both with b_1 symmetry. Interestingly, the splitting when pyrimidine is interacting with silver is much less than observed in neat pyrimidine.

When comparing the three Raman spectra of bulk pyrimidine, pyrimidine-water solution, and pyrimidine-methanol solution the same trend is apparent as described with ν_{6a} and ν_{6b} in which a large blue shift is observed with the pyrimidine-water mixture compared with the pyrimidine-methanol solution. This effect is again attributed to the greater probability of pyrimidine and water forming hydrogen bonds. However, when analyzing the SERS spectra, the interaction among silver, pyrimidine, and solvent molecules becomes apparent.

The ν_1 mode of the pyrimidine SERS spectrum is fit with three Lorentzian functions and is shown in Figure 3.4. Lorentzian fits for ν_1 are also shown in Figure 3.5 and Figure 3.6 for the pyrimidine-water SERS and pyrimidine-methanol SERS, respectively. The Lorentzian functions are used to show the distribution of three possible interactions.

The lowest energy shoulder corresponds to the pyrimidine with no chemical interactions with the SERS substrate - which will be further denoted as free pyrimidine. The center peak corresponds to one of pyrimidine's nitrogen atoms interacting with silver, and the largest energy peak on the right denotes both of pyrimidine's nitrogen atoms interacting with silver. The energies of these three regions of ν_1 are tabulated in Table 3.3.

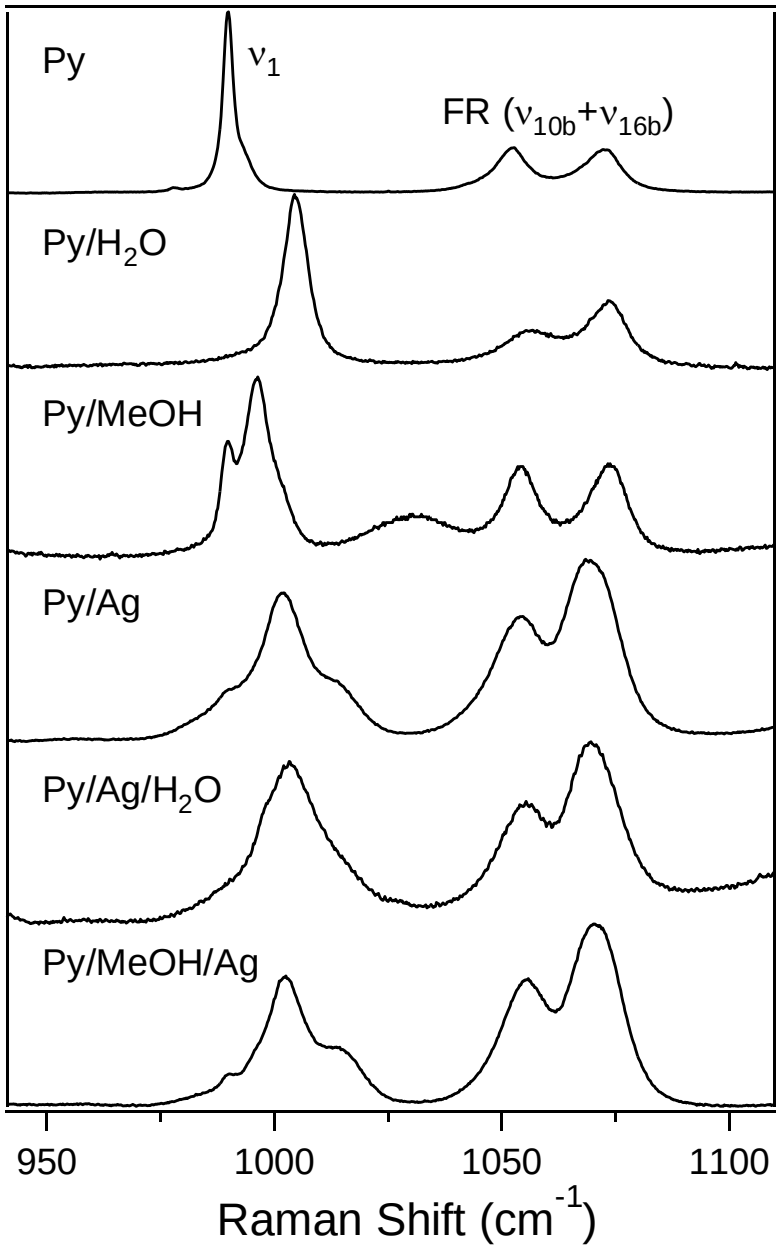

Figure 3.3 Spectral region showing evolution of ν_1 and the Fermi resonance of $\nu_{10b} + \nu_{16b}$.

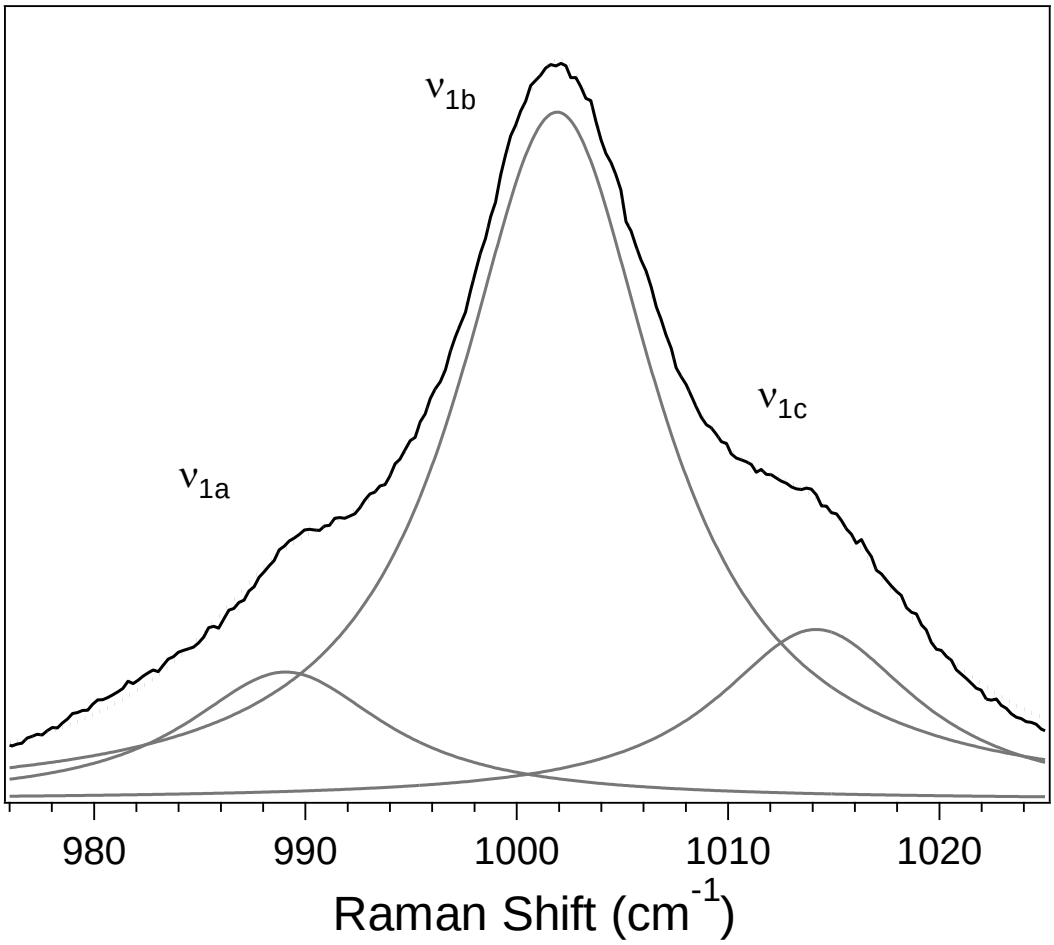

Figure 3.4 Pure pyrimidine SERS spectrum with a curve fit of 3 Lorentzian functions.

ν_1	pyr-Ag	pyr-H_2O-Ag	pyr-MeOH-Ag
ν_{1a} (left)	989	-	990
ν_{1b} (center)	1002	1003	1002
ν_{1c} (right)	1015	1015	1015

Table 3.3 Lorentzian functions of ν_1 showing the three distinct regions of interactions.

As can be seen from the data of Table 3.3, the lowest energy peak, ν_{1a} is essentially of the same energy as the ν_1 mode of the pure pyrimidine Raman spectrum - which only corresponds to pyrimidine-pyrimidine interactions (free pyrimidine). This energy match

indicates that the pyrimidine molecule is not interacting with the SERS substrate. The central peak of this mode, ν_{1b}, has the greatest relative intensity. Pyrimidine contains two nitrogen atoms; since this central peak is of greater intensity it can be deduced that it illustrates one of the pyrimidine nitrogen atoms interacting with the silver substrate. There is a larger probability of the silver atoms interacting with one of the two nitrogen atoms and a lower probability of silver interacting with both or neither of the nitrogen atoms. The larger probability of possible interactions explains the greater relative intensity of $\nu_{1b.}$ The largest energy mode, ν_{1c}, indicates the silver interactions on both of the nitrogen atoms as mentioned previously.

Figure 3.5 and Figure 3.6 shows the results of the Lorentzian curve fits of ν_1 for the pyrimidine-water SERS and pyrimidine-methanol SERS respectively. It can be seen from Figure 3.5, that the pyrimidine-water mixture does not experience the same interactions during the acquisition of the SERS spectrum when comparing it to Figure 3.4 and Figure 3.6. In the pyrimidine-water SERS spectrum, the two shoulders ν_{1a} and ν_{1c} are masked by the pyrimidine interacting with the hydrogen molecules. ν_{1c} is only present once the Lorentzian fits are performed. The absence of a definitive ν_{1a} peak is indicative of the hydrogen bonded networks formed with the water and pyrimidine molecules, and it shows the competition between pyrimidine-water and pyrimidine-pyrimidine interactions since ν_{1a} represents neat pyrimidine with no interactions. On the other hand, methanol is also capable of hydrogen bonding with pyrimidine, but Figure 3.6 shows a definitive ν_{1a} peak. This phenomenon can be attributed to the lesser degree of hydrogen bonding of methanol as compared to water so essentially free pyrimidine is being detected.

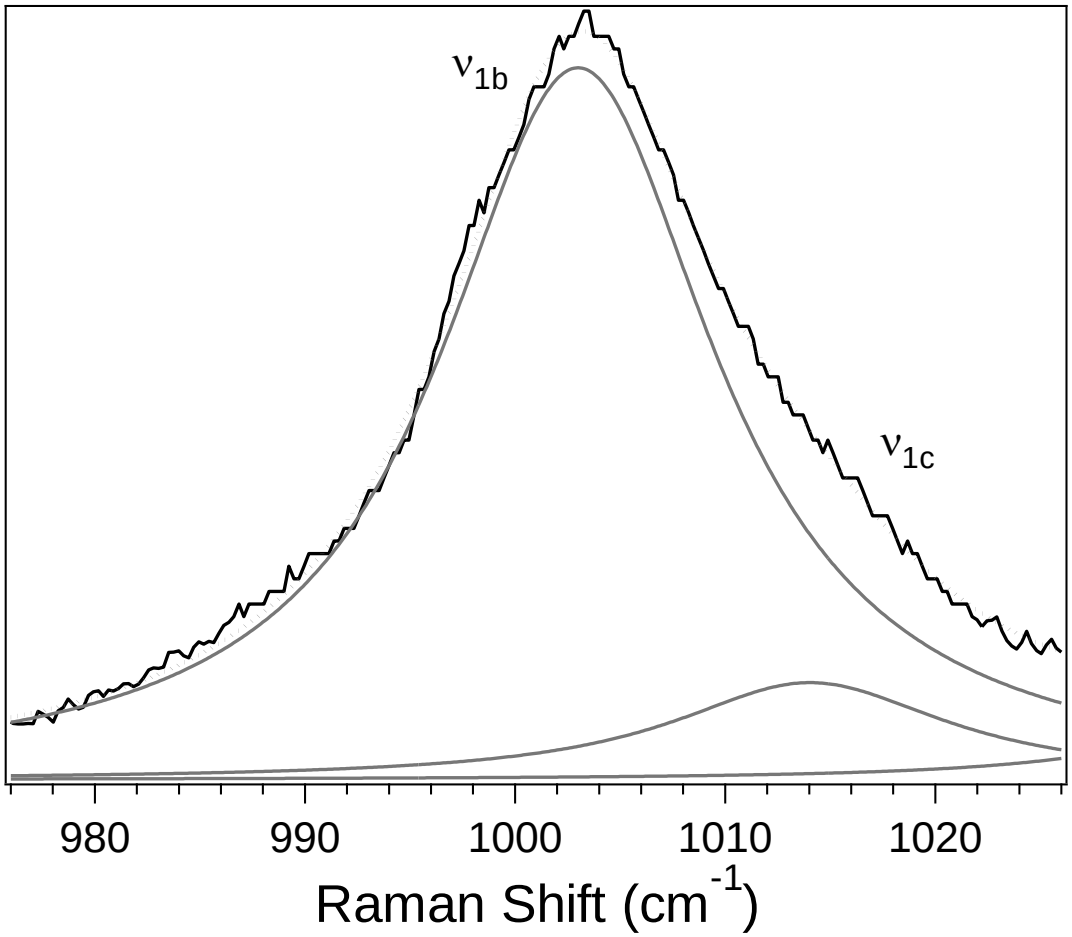

Figure 3.5 1M pyrimidine solution SERS spectrum fit with Lorentzian functions.

Interestingly, ν_{1c} is the same for all three solutions indicating that the presence of solvent does not affect the interactions between the silver SERS substrate and the two nitrogen atoms of the pyrimidine molecules. When comparing the Raman shifts of Table 3.3, each peak associated with ν_1 has the same energy independent of the solution which can allude to the competition of charge transfer from the silver substrate or from the water molecules to the pyrimidine. These results suggest that charge transfer from the silver substrate dominates the interactions since the spectral shifts of the totally symmetric mode are the same whether interacting with silver, water, or methanol and it was previously demonstrated that charge transfer is the origin of this blue shifting.

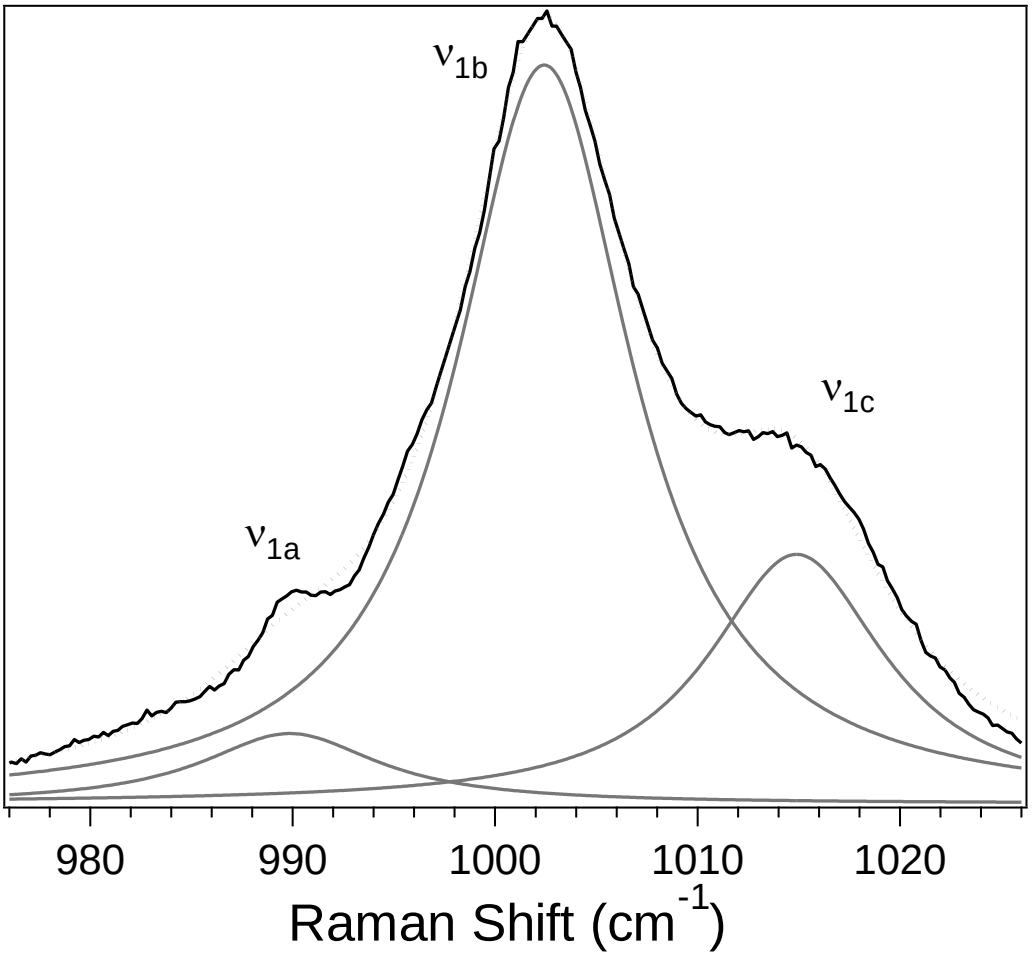

Figure 3.6 Pyrimidine-methanol solution SERS spectrum fit with 3 Lorentzian functions.

3.3.4 Modes ν_{8a} and ν_{8b}

The last region of the pyrimidine spectrum studied in detail is depicted in Figure 3.6. This region shows the modes ν_{8a} and ν_{8b}, a CN stretch and CC/CN stretch respectively. As previously reported by Howard et al., ν_{8a} and ν_{8b} experience different degrees of shifting with increasing mole fractions of water with a shift of +6 for ν_{8a} and +12 for ν_{8b}. Our results confirm these shifts when comparing the Raman spectra of pyrimidine and pyrimidine-water. The pyrimidine-methanol solution does not show as great of spectral shifts in the Raman spectra since methanol is not as strong of a hydrogen bonding solvent as water.

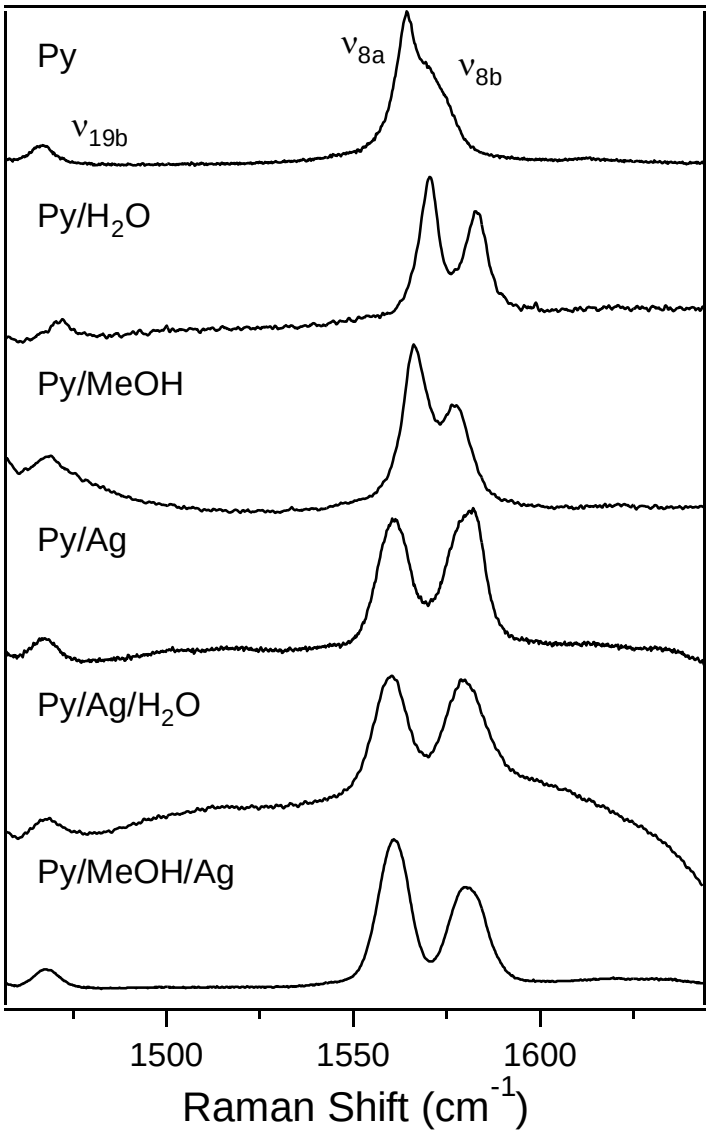

Figure 3.7 Evolution of ν_{8a} and ν_{8b} analyzed with Raman and SERS spectra.

The SERS spectra of this region show ν_{8a} and ν_{8b} splitting without the added interactions of the solvent. Comparing the magnitude of the shifts in Table 3.2, the shifts of ν_{8a} and ν_{8b} are fairly constant when comparing the 3 SERS spectra while they exhibit different magnitudes of blue shifting with the Raman spectra of the two solutions. The hydrogen bonding effect of the solvents results in the shifting variation of the normal

modes in the Raman spectra; in the SERS spectra, however, since the shifts are occurring at the same magnitude it can be inferred that the charge transfer interactions of silver with the pyrimidine are causing the modes to shift and dominate over the hydrogen bonding from the solvent. The solvent interactions are not affecting the energies of ν_{8a} and ν_{8b} since charge transfer from silver is present. These two modes involve the vibrational movement of a nitrogen atom. Since the nitrogen atoms of the pyrimidine ring contain a lone pair of electrons, the one unpaired electron of silver readily participates in charge transfer interactions causes the experimental shifts of ν_{8a} and ν_{8b}.

As previously reported, ν_{8a} and ν_{9a} exhibit similar vibrational motions. These two modes show a slight red shift in the pure pyrimidine SERS spectrum. This experimental shift to lower energies is an effect of the charge transfer mechanism between the silver and adsorbate. ν_{16a} also exhibits a red shift in the pure pyrimidine SERS. Interestingly, only ν_{8a} and ν_{16a} continue to show a red shift in the SERS spectra of pyrimidine solutions. Since the red shift is still present even though there are possible interactions with either water or methanol available, the silver charge transfer interactions with pyrimidine affects these two modes and is favored over the intermolecular interactions with the solvent.

3.3.5 Comparison to Theory

In chemistry as well as other science fields, it is imperative to include computational data to model the experimental results acquired during a study. As part of this project, Dr. Ashley Wright studied the interactions between pyrimidine and silver using Density Functional Theory (DFT) computations. The Gaussian 09 program was used for the

calculations. The B3LYP/6-311++G(2*d*,2*p*)/LanL2DZ level of theory was used to calculate the harmonic vibrational frequencies. The vibrational shifts of the normal modes of pyrimidine interacting with water, silver, or both as compared to the pyrimidine monomer are listed in Table 3.3. The optimized structures of the computational results are illustrated in Figure 3.8.[37]

Mode	pyr (cm^{-1})	1w + 0	Ag_2 + 0	Ag_2 + Ag_2	Ag_2 + 1w
ν_{6b}	637.7	+4	+9	+19	+15
ν_{6a}	696.9	+4	+2	+1	+4
ν_{1}	1009.6	+8	+11	+19	+17
ν_{9a}	1082.7	+1	+2	+4	+2
ν_{3}	1400.3	+1	+2	+2	+3
ν_{8a}	1607.1	-1	-4	+3	+1
ν_{8b}	1606.1	+9	+14	+15	+15

Table 3.3 Vibrational shifts of normal modes of pyrimidine interacting with silver and/or water compared with the pyrimidine monomer.[37]

Here, the theoretical results are a close match to the experimental data reported earlier in this thesis. By comparing the theoretical shifts of ν_1, the interactions of the nitrogen atoms on pyrimidine can be further verified. Experimentally, a shift of +13 occurs from ν_{1a} to ν_{1b}. These two peaks correspond to the theoretical data of the pyrimidine mode and Ag_2 + 0 shift. The shift to Ag_2 + 0 for ν_1 is +11; the similarity of computational shift to experimental shift suggests that ν_{1b} corresponds to silver interacting with only one of the nitrogen atoms. The same trend is apparent with the comparison of Ag_2 + Ag_2 to ν_{1c} further verifying our conclusion that ν_{1c} corresponds to silver atoms interacting with both nitrogen atoms of the pyrimidine ring.

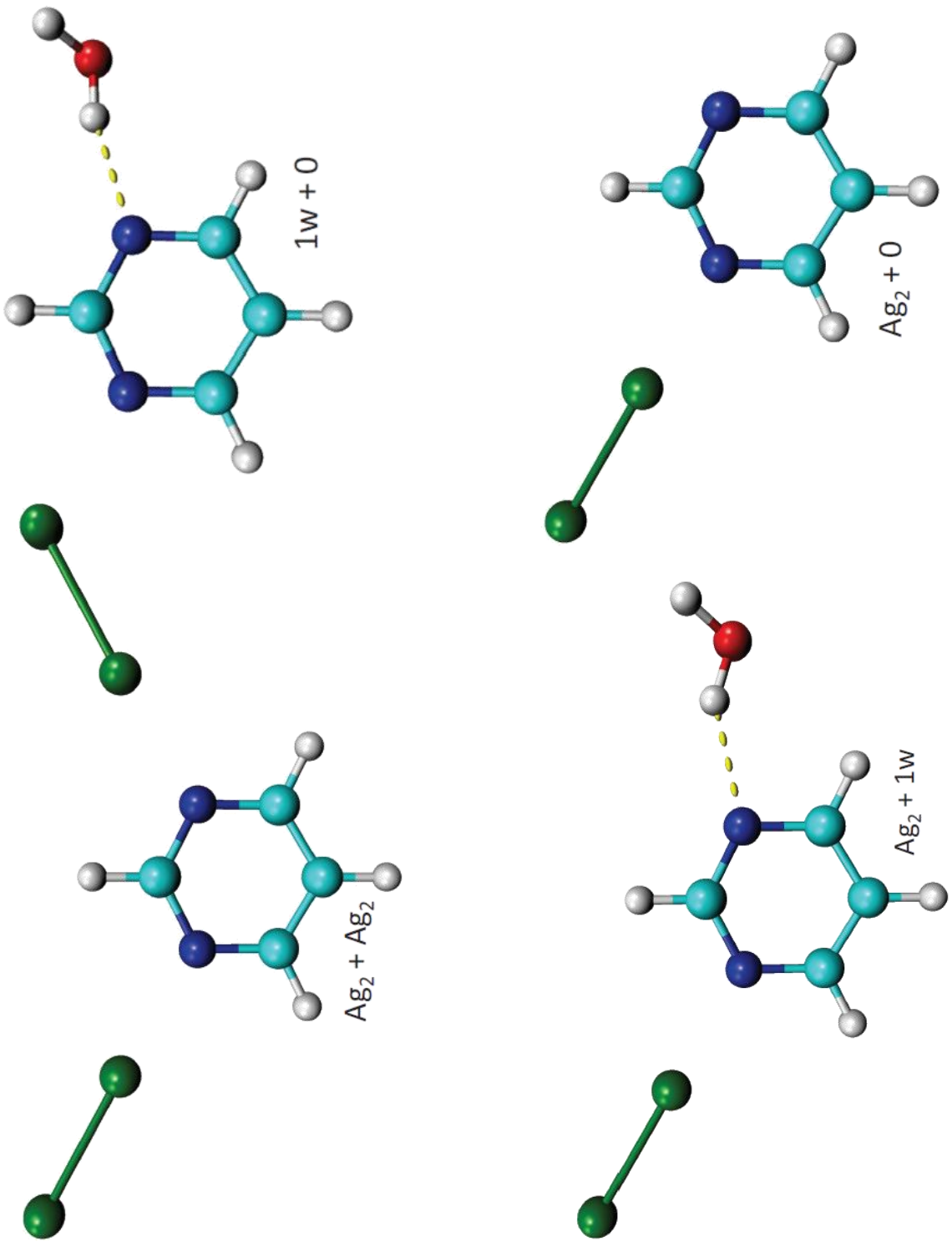

Figure 3.8 Optimized molecular clusters of pyrimidine, silver, and water.[37]

The experimental shifts of pyrimidine modes ν_{8a} and ν_{8b} can also be further explained by the computational results. Experimental data from previous publications as well as data from this study show blue shifts of ν_{8a} and ν_{8b} when hydrogen bonded networks form between the pyrimidine and solvent; however, the interactions with silver cause variations in these shifts. By comparing the magnitude of these shifts from the interactions with silver, it can be seen from Table 3.2 and Table 3.3 that the shifting is held fairly constant when silver interacts with the adsorbed pyrimidine. The correlation between computational and experimental data then verifies the results of charge transfer with silver.

Wright, et al. recently reported that the magnitude of the Raman shift in pyrimidine due to hydrogen bonded interactions with the nitrogen atoms is directly proportional to the magnitude of charge transfer.[39] Comparison to the calibration curve of Raman shift as a function of charge transfer for pyrimidine interacting with silver suggests a charge transfer of 35 me and 80 me for the two bonded components in ν_1. Natural bond orbital (NBO) calculations on the Py/Ag and Py/Ag/Solvent complexes will follow for a confirmation of these results.

3.4 Conclusions

Comparison of the experimental Raman spectrum of pyrimidine to the Raman and SERS spectra of pyrimidine, pyrimidine-water, and pyrimidine-methanol mixtures suggests that the controversial chemical enhancement of the SERS substrate exists in this system. The silver molecules interact with the nitrogen atoms of pyrimidine resulting in a variation of shifting for the modes ν_1, ν_{8a}, and ν_{8b}. These pyrimidine modes exhibit the most variation

since their motions greatly depend on the positioning of the nitrogen atoms in the molecular structure. The SERS substrate, therefore, is able to interact with the lone pairs on these nitrogen atoms most affectively influencing the shifting of these three modes to the greatest degree. There is a competition in charge transfer, therefore, between pyrimidine and silver and pyrimidine and the hydrogen bonded solvent molecules. Spectral shifts suggest that interactions with silver dominate. The magnitude of the Raman shift suggests charge transfer from pyrimidine to the silver atoms on the order of 35 me and 80 me for interacting with one or both nitrogen atoms, respectively.

List of References

(1) McHale, J. L. *Molecular Spectroscopy*, **1999**.

(2) Bernath, P.F. *Spectra of Atoms and Molecules*, **2005.**

(3) Engel, T.; Reid, P. *Physical Chemistry*, **2010**.

(4) Raman, C.V., *Nature*, **1928**.

(5) Garland, C. W.; Nibler, J.W.; *Experiments in Physical Chemistry*, **2009**.

(6) Robinson, J.W.; Skelly Frame, E.M.; Frame II, G.M. *Undergraduate Instrumental Analysis*, **2005**.

(7) Le Ru, E.C.; Etchegoin, P.G. *Principles of Surface-Enhanced Raman Spectroscopy and Related Plasmonic Effects*, **2009**.

(8) Joule, J.A.; Mills, A. *Heterocyclic Chemistry,* **2010**.

(9) Alvarez-Builla, J.; Vaquero, J.J.; Barluenga, J. *Modern Heterocyclic Chemistry*, **2011**.

(10) Johnson, T.B. *Journal of Industrial and Engineering Chemistry*, **1918**, 10, 4, 306-312.

(11) Jain, K.S.; Chitre, T.S.; Miniyar, P.B.; Kathiravan, M.K.; Bendre, V.S.; Veer, V.S.; Shahane, S.R.; Shishoo, C.J. *Current Science*, **2006**, 90, 6, 793-803.

(12) Khurana, I. *Textbook of Human Physiology for Dental Students*, **2007**.

(13) Duggan, C.; Watkins, J.B.; Walker, W.A. *Nutrition in Pediatrics: Basic Science, Clinical Applications*, **2008**.

(14) Howard, A.A.; Tschumper, G.S.; Hammer, N.I. *J. Phys. Chem. A.*, **2010**, 114, 6803-6810.

(15) Howard, J.C.; Hammer, N.I.; Tschumper, G.S. *ChemPhysChem*, **2011**, 12, 3262-3273.

(16) Wright, A.M.; Joe, L.V.; Howard, A.A.; Tschumper, G.S.; Hammer, N.I. *Chem. Phys. Letters*, **2011**, 501, 319-323.

(17) Centeno, S.P.; López-Tocón, I.; Arenas, J.F.; Soto, J.; Otero, J.C. *J. Phys. Chem. B.*, **2006**, 110, 14916-14922.

(18) Jeanmaire, D.; Van Duyne, R. *Journal of Electroanalytical Chemistry*, **1977**, 84, 1-20.

(19) Albrecht, M.G.; Creighton, J.A. *J. Am. Chem. Soc.*, **1977**, 99, 15, 5215-5217.

(20) Doering, W.; Nie, S. *Anal. Chem.*, **2003**, 75, 6171-6176.

(21) Grubisha, D.S.; Lipert, R.J.; Park, H.Y.; Driskell, J.; Porter, M.D. *Anal. Chem.*, **2003**, 75, 21 5936-5943.

(22) Barhoumi, A.; Zhang, D.; Tam, F.; Halas, N.J. *J. Am. Chem. Soc.*, **2008**, 130, 5523-5529.

(23) Sha, M.Y.; Xy, H.; Natan, M.J.; Cromer, R. *J. Am. Chem. Soc.*, **2008**, 130, 17214-17215.

(24) Corrigan, D.K.; Cauchi, M.; Piletsky, S. *PDA J. Pharm. Sci. and Tech.*, **2009**, 63, 568-574.

(25) Kneipp, K.; Wang, Y.; Kneipp, H.; Perelman, L.T.; Itzkan, I.; Dasari, R.R.; Feld, M.S. *Phys. Rev. Lett.* **1997**, 78, 1667-1670.

(26) Nie, S.; Emory, S.R. *Science*, **1997**, 275, 1102-1106.

(27) Kneipp, K.; Kneipp, H.; Itzkan, I.; Dasari, R.R.; Feld, M.S. *Chemical Reviews,* **1999**, 99, 2957-2976.

(28) Etchegoin, P.G.; Le Ru, E.C. *Phys. Chem. Chem. Phys*., **2008**, 10, 40, 6079-6089.

(29) Schlucker, S. *Chem. Phys. Chem*., **2009**, 10, 1344-1354.

(30) El-Ansary, A.; Faddah, L.M. *J. Nanotech. Sci. and App*. **2010**, 3, 65-76.

(31) Nibbering, E.T.J.; Elsaesser, T.; *Chemical Reviews,* **2004**, 104, 4, 1887-1914.

(32) Hering, K.; Cialla, D.; Ackermann, K.; Dörfer, T.; Möller, R.; Schneidewind, H.; Mattheis, R; Fritzsche, W.; Rösch, P.; Popp, J. *Anal. and Bioanal. Chem*. **2008**, 390, 113-124.

(33) Bakker, H.J.; Skinner, J.L. *Chemical Reviews,* **110**, 3, 1498.

(34) Edward, A.G.S. *Nature (London),* **2002**, 477, 39.

(35) Muniz-Merando, M.; Cardini, G.; Schettino, V. *Theor. Chem. Acta*, **2004**, 111, 264-269.

(36) te Velde, G.; Bickelhaupt, F.M.; Baerends, E.J.; Fonseca Guerra, C.; van Gisbergen, S. J. A.; Snijders, T. G.; Ziegler, T. *J. Comp. Chem.* **2001**, 22, 931.

(37) Wright, A. *Investigations of Noncovalent Interactions Using Raman Spectroscopy and Electronic Structure Computations.* Ph.D. Dissertation, University of Mississippi, 2012.